Supporting Information: Tuning fast excited-state decay by lignad attachment in isolated chlorophyll *a*

Elisabeth Gruber, Ricky Teiwes, Christina Kjær, Steen Brøndsted Nielsen and Lars H. Andersen

EXPERIMENT

Photo-dissociation studies after excitation into the Q and Soret (B) bands, performed by ns-laser pulses at the ion-storage ring ELISA [1]

Besides the impact of the ligand on the spectroscopic properties, we observe large differences in the fragmentation behavior between the chl*a*-TMA and the chl*a*-formate complexes. The differences are ascribed to different binding energy in the two Chl*a* systems. A loosely bound system may fragment after absorption of a single photon, whereas a tighter bound system may require more photons to fragment and hence cause detectable action. Likewise, absorption of two or more photons gives a much faster event (higher dissociation rate) than absorption of a single photon does.

After excitation, the molecular system eventually relaxes by non-radiative decay channels into a vibrationally hot electronic ground state. From there, the molecular system with high internal energy undergoes fast intra-molecular energy redistribution followed by statistical fragmentation, when ignoring slow radiative cooling [2].

In Fig. 1, the photofragment yield is shown as a function of time and of the laser-pulse energy for both complexes after excitation into the Q and Soret bands (640-660 nm and 395-430 nm). For the chl*a*-TMA complex we observe prompt dissociation (red signal) as well as delayed dissociation over a time scale of several ms (blue signal). The chl*a*-formate data show almost exclusively prompt action. Prompt action is defined as fragmentation within the first 20 μs (a quarter revolution time in the ring), whereas delayed action is associated with fragmentation from 40 μs up to several ms after photoabsorption.

The yield of delayed action nicely follows a Poisson distribution for single-photon absorption (n=1). Prompt action, on the other hand, is caused by sequential multiphoton absorption which is

in agreement with observations obtained in single-pass experiments [3].
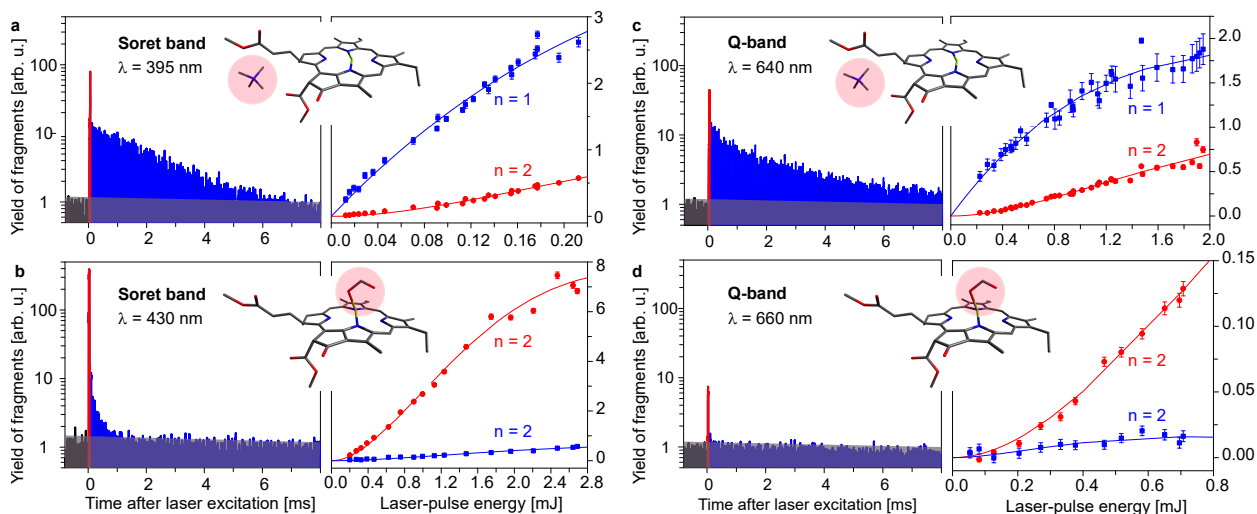
Figure 1. **Photo-dissociation studies at the ELISA ion-storage ring**

Histograms of neutral photo fragments as a function of time for the chla-TMA complex (a,c) and for the chla-HCOO$^-$ complex (b,d) after excitation into the Soret band (a,b) and the Q band (c,d) by ns laser pulses in the storage ring ELISA. The shadowed grey area represents the background fragmentation, induced by collision with the rest gas in the storage ring. The fitting of the fragmentation yield as a function of laser-pulse energy was done using Poisson statistics. *n* corresponds to the number of independent photons absorbed within one ns laser pulse.

CALCULATIONS

Structure and energy calculations of chl*a*

Vertical energies of chl*a* are obtained through DFT calculations by the Gaussian16 software package [4] using the ωB97XD functional and TZVP basis. The structure of chl*a* is optimized at the same level of theory. For comparison, we also optimize the structure by PM3, which only gives slightly different excited-state energies, with shifts between 0.01 - 0.1 eV. The B3LYP functional gives some changes to the energy for T_1 where the energy is shifted to 1.39 eV, and for S_2 which is shifted to 2.35 eV. The other states have very small changes. We note that the DFT method may not fully capture the charge-transfer character of the involved transitions and as a consequence they do not completely reproduce the spectroscopy of chl*a*. Moreover, we use a model chlorophyll without the phytyl tail of Chl$_a$, which might also contribute to small changes in spectroscopy.
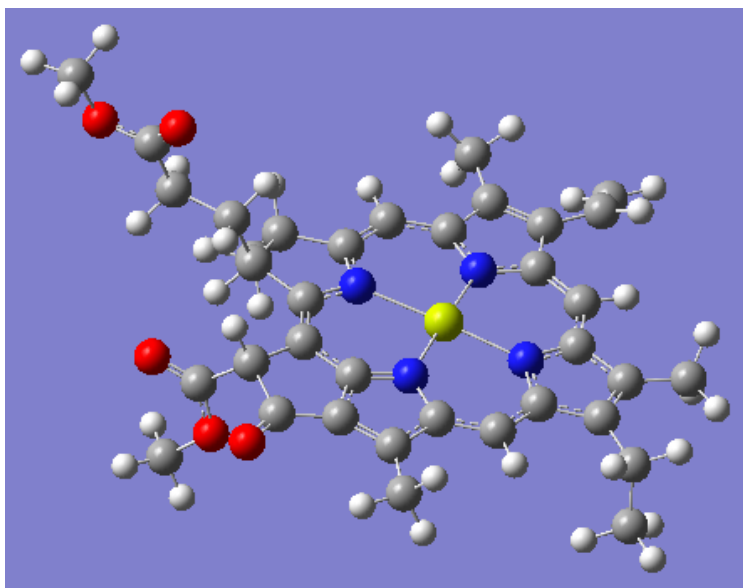

Figure 2. **DFT optimized structure of Chl***a*

Chlorophylla DFT optimized (ωB97XD/TZVP)

Atom	x	y	z	Atom	x	y	z
C	-5.59982100	3.44040400	0.65730200	Mg	-7.24320600	0.94984600	-0.16776900
C	-5.96400200	4.87391400	0.74336600	C	-11.95587700	3.08282000	-1.56267400
C	-7.27111200	4.99176900	0.38046700	H	-12.16830400	3.62192400	-0.63005700
C	-7.76634500	3.62297500	0.02183700	H	-11.61681300	3.81825400	-2.30423000
C	-9.04325800	3.45593600	-0.43469300	H	-12.89753700	2.63722800	-1.92629000
C	-9.60125300	2.22443600	-0.82645700	C	-12.79436200	-1.15224700	-1.47035900
C	-10.95018700	2.02946700	-1.35529800	H	-12.02468900	-1.94244400	-1.44154700
C	-11.10331300	0.68546300	-1.62760700	H	-13.05201800	-0.90780200	-0.43229300
C	-9.86248600	0.02164600	-1.26086200	H	-13.68857100	-1.57712200	-1.94298000
C	-9.51529000	-1.30635500	-1.30627600	O	-5.36176300	-5.27453100	-0.34826900
C	-8.25513800	-1.75802800	-0.89351500	H	-1.90302200	1.51920600	0.56711300
C	-7.84511700	-3.14216900	-0.93034000	C	-2.22637900	1.46268600	2.69717600
C	-6.55440700	-3.17367500	-0.43379600	H	-2.18816800	2.55301500	2.82360000
C	-6.18737900	-1.82189300	-0.09447000	H	-2.92090900	1.06848600	3.45083500
C	-4.83574800	-1.78385900	0.40360600	H	-1.22813300	1.06573900	2.92764000
C	-4.18413200	-0.63742800	0.67299800	C	-1.77590900	-1.00464600	0.06569300
C	-2.75085400	-0.45072800	1.10315800	C	-0.37051400	-1.10246300	0.63631000
C	-2.63759200	1.08420100	1.28838200	H	-1.78190100	-0.38037900	-0.85007300
C	-4.02439300	1.58299000	0.92737400	H	-2.12403100	-2.01390700	-0.25868500
C	-4.36346500	2.96079800	0.97046300	C	0.63988600	-1.54766200	-0.39527600
N	-6.73631400	2.69678500	0.21494600	H	-0.05849200	-0.12305400	1.05625500
N	-8.97514600	1.02677800	-0.78201900	H	-0.35044100	-1.81676600	1.48610900
N	-7.18673100	-0.94080900	-0.36903000	O	0.45326100	-1.88622900	-1.54743400
N	-4.87937900	0.62068500	0.56617900	O	1.91213000	-1.54237500	0.10079900
H	-9.69371600	4.34450600	-0.51982800	C	2.97603600	-1.96879900	-0.75461600
H	-10.26167000	-2.04027800	-1.65939500	H	3.01711700	-1.32003800	-1.65255300
H	-3.57977700	3.66360600	1.28588600	H	2.79361400	-3.00808800	-1.09266200
H	-2.58619400	-0.97985100	2.07524500	C	-12.30302100	0.06124400	-2.22864600
C	-4.99814600	5.90526900	1.15635700	H	-13.10125800	0.83800700	-2.28642300
C	-7.88051800	7.35340400	0.81381900	H	-12.06906500	-0.21212400	-3.27742400
C	-8.65222900	-4.27431300	-1.40857300	C	-8.13179500	6.15202300	0.29740900
C	-5.44746800	-4.08317200	-0.15146700	H	-9.08175000	5.97281400	-0.23571100
H	-5.41439400	6.92150300	1.08046600	C	-4.31061100	-3.20261300	0.45288800
H	-4.09532700	5.86832900	0.53052700	C	-3.94297700	-3.62325100	1.86652900
H	-4.68814600	5.75102100	2.19959300	O	-2.81803300	-3.69195900	2.32480000
H	-6.97122100	7.59998600	1.36089700	O	-5.00400800	-3.93245400	2.66360600
H	-8.57955400	8.17895400	0.71911800	C	-4.75600000	-4.37103800	3.98280500
H	-9.60436200	-4.33849000	-0.86370400	H	-5.76535100	-4.55831500	4.35781800
H	-8.12438800	-5.22785500	-1.27838400	H	-4.16217700	-5.29106600	4.00247000
H	-8.88785300	-4.16312500	-2.47609300	H	-4.26185800	-3.59836500	4.58133400
				H	-3.38565100	-3.26391600	-0.18317400
				H	3.87778723	-1.89765434	-0.18305397

Figure 3. **DFT optimized structure of Chl***a*

4

SOC: Chl*a* ωB97XD/TZVP (ωB97XD/TZVP optimized)

```
Excited state symmetry could not be determined.
Excited State   1:      Triplet-?Sym    1.0208 eV 1214.55 nm  f=0.0000  <S**2>=2.000
     165 -> 167       0.21847
     165 -> 168       0.19600
     166 -> 167       0.67174
     166 -> 168      -0.13531
     165 <- 168       0.12434
     166 <- 167       0.24166
This state for optimization and/or second-order correction.
Total Energy, E(TD-HF/TD-DFT) = -2188.86539498
Copying the excited state density for this state as the 1-particle RhoCI density.

Excited state symmetry could not be determined.
Excited State   2:      Triplet-?Sym    1.6096 eV  770.30 nm  f=0.0000  <S**2>=2.000
     165 -> 167       0.63342
     166 -> 167      -0.24621
     166 -> 168      -0.18082
     165 <- 167       0.15548

Excited state symmetry could not be determined.
Excited State   3:      Triplet-?Sym    2.0758 eV  597.29 nm  f=0.0000  <S**2>=2.000
     160 -> 167       0.11442
     165 -> 167       0.18072
     165 -> 168       0.13080
     166 -> 168       0.64122

Excited state symmetry could not be determined.
Excited State   4:      Singlet-?Sym    2.1468 eV  577.53 nm  f=0.2187  <S**2>=0.000
     165 -> 168       0.26683
     166 -> 167       0.63645

Excited state symmetry could not be determined.
Excited State   5:      Singlet-?Sym    2.5785 eV  480.85 nm  f=0.0404  <S**2>=0.000
     165 -> 167       0.56547
     166 -> 167      -0.12370
     166 -> 168      -0.38737
```

```
Excited state symmetry could not be determined.
Excited State   6:      Triplet-?Sym    2.5979 eV  477.25 nm  f=0.0000  <S**2>=2.000
     165 -> 167      -0.10189
     165 -> 168       0.61530
     165 -> 169      -0.15727
     166 -> 167      -0.15260

Excited state symmetry could not be determined.
Excited State   7:      Triplet-?Sym    2.7327 eV  453.70 nm  f=0.0000  <S**2>=2.000
     163 -> 167       0.44916
     163 -> 168       0.26765
     163 -> 169       0.17204
     163 -> 170      -0.16917
     164 -> 167      -0.28902
     164 -> 168      -0.13667
     164 -> 169      -0.10003

Excited state symmetry could not be determined.
Excited State   8:      Singlet-?Sym    3.4814 eV  356.13 nm  f=0.9756  <S**2>=0.000
     163 -> 167       0.14848
     165 -> 167       0.36718
     166 -> 168       0.56531

Excited state symmetry could not be determined.
Excited State   9:      Singlet-?Sym    3.7176 eV  333.50 nm  f=0.3447  <S**2>=0.000
     163 -> 167      -0.41245
     163 -> 168      -0.18670
     164 -> 167       0.41877
     165 -> 167       0.11076
     165 -> 168       0.22071

Excited state symmetry could not be determined.
Excited State  10:      Singlet-?Sym    3.7584 eV  329.89 nm  f=0.8134  <S**2>=0.000
     163 -> 168       0.10802
     164 -> 167      -0.20020
     165 -> 168       0.57838
     166 -> 167      -0.25595
```

Figure 4. **DFT energies of Chl*a***

Table I. Transition energies and oscillator strength calculated for chl*a* with Gaussian16 using TDDFT with the ωB97XD functional and TZVP basis. The structures are obtained at the same level of theory.

Excited State	Multiplicity	Transition Energy(eV)	Wavelength(nm)	Oscillator Strength
Excited State 4	Singlet	2.1468	577.53	0.2187
Excited State 5	Singlet	2.5785	480.85	0.0404
Excited State 8	Singlet	3.4814	356.13	0.9756
Excited State 9	Singlet	3.7176	333.50	0.3447
Excited State 10	Singlet	3.7584	329.89	0.8134
Excited State 1	Triplet	1.0208	1214.55	0.0000
Excited State 2	Triplet	1.6096	770.30	0.0000
Excited State 3	Triplet	2.0758	597.29	0.0000
Excited State 6	Triplet	2.5979	477.25	0.0000
Excited State 7	Triplet	2.7327	453.70	0.0000
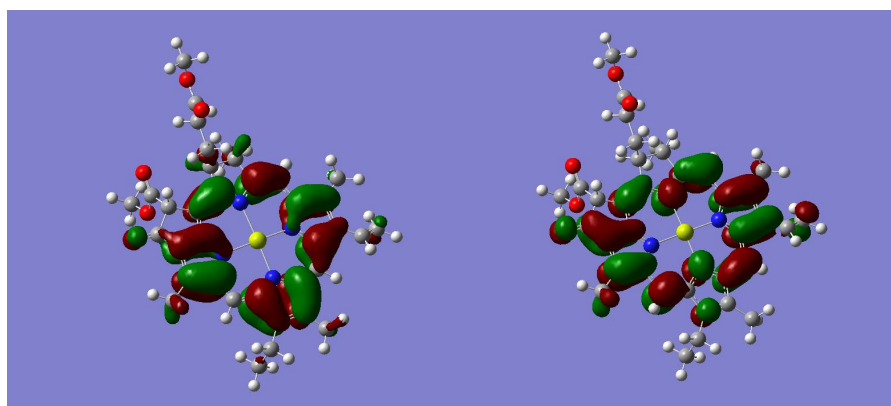
Homo orbital (166) of Chla.   Lumo orbital (167) of Chla.

Figure 5. **Molecular orbitals of Chl*a***

ωB97XD/TZVP//PM3

S₂	2.65 eV (467 nm)
S₁	2.13 eV (581 nm)

T₃ 1.99 eV
T₂ 1.73 eV
T₁ 1.01 eV

S₀ 0.00 eV

ωB97XD/TZVP//ωB97XD

S₂	2.58 eV (481 nm)
S₁	2.14 eV (578 nm)

T₃ 2.08 eV
T₂ 1.61 eV
T₁ 1.02 eV

S₀ 0.00 eV

B3LYP/6-311++G(d,p)//ωB97XD

S₂	2.35 eV (528 nm)
S₁	2.17 eV (572 nm)

T₃ 2.09 eV
T₂ 1.64 eV
T₁ 1.39 eV

S₀ 0.00 eV
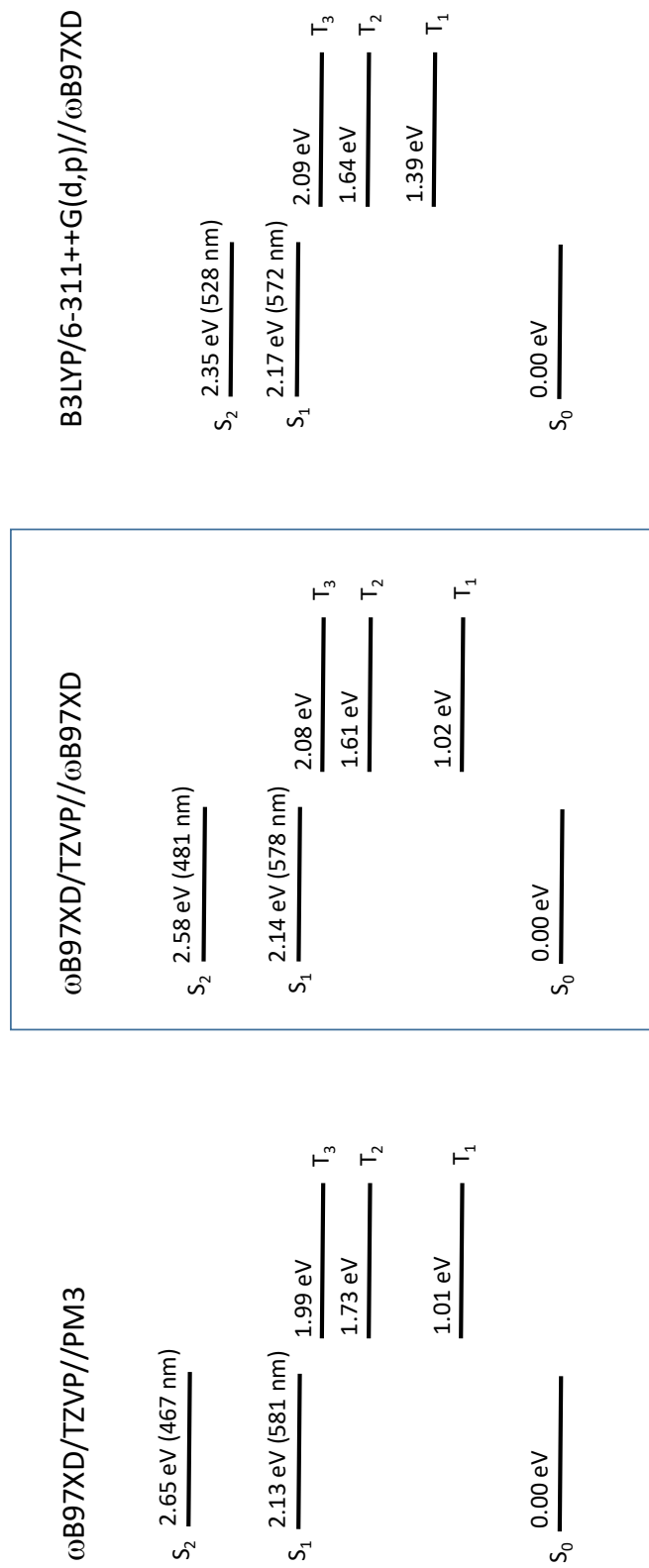
Results in the box are used for the SOC calculation

Figure 6. **Chl*a* spectroscopy summary**

Structure and energy calculations of chl*a*-formate

Vertical energies of chl*a*-formate are obtained through DFT calculations by the Gaussian16 software package [4] using the ωB97XD functional and TZVP basis. The structure of the chl*a*-formate complex is optimized at the same level of theory. For comparison, we also optimize the structure by PM3, which only gives slightly different excited-state energies, with shifts between 0.01 - 0.13 eV. The B3LYP functional gives some changes to the energy for T_1 where the energy is shifted to 1.36 eV, and for S_2 which is shifted to 2.19 eV. The other states have very small changes. We note that the DFT method may not fully capture the charge-transfer character of the involved transitions and as a consequence they do not completely reproduce the spectroscopy of chl*a*-formate.

Figure 7. **DFT optimized structure of Chl*a*-formate**

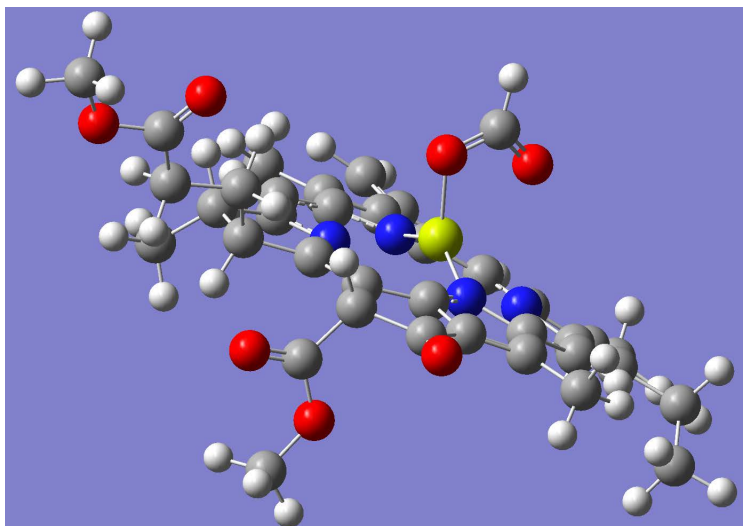Chlorophyll *a* – formate DFT optimized (ωB97XD/TZVP)

Atom	X	Y	Z
C	-1.2165600	3.0229020	0.6103730
C	-2.0761970	4.1926910	0.8098530
C	-3.3511430	3.7641330	0.6258760
C	-3.2718200	2.3355530	0.3055440
C	-4.3468700	1.5199060	0.0849180
C	-4.3361260	0.1227580	-0.1593050
C	-5.5188700	-0.7064630	-0.2522200
C	-5.0766480	-1.9854220	-0.4234770
C	-3.6300080	-1.9203190	-0.4258460
C	-2.7716570	-3.0043700	-0.4893700
C	-1.3764730	-2.9757880	-0.3940990
C	-0.4898400	-4.0958380	-0.3298890
C	0.7729310	-3.5355210	-0.1779750
C	0.5897820	-2.1343030	-0.1603520
C	1.7895890	-1.3996190	0.0284150
C	1.8541560	-0.0596700	0.2314020
C	3.1043200	0.7391440	0.5348130
C	2.5332200	2.1130660	0.9352640
C	1.0527660	1.9749190	0.6037760
C	0.1759320	3.0436250	0.7421020
N	-1.9580440	1.9477860	0.3138000
N	-3.2307580	-0.6153140	-0.2793600
N	-0.6735350	-1.7881650	-0.2914230
N	0.7374590	0.7392790	0.2267440
H	-5.3253880	1.9819370	0.1351490
H	-3.2288300	-3.9842010	-0.5836610
H	0.6211350	1.0236270	1.3859830
H	3.6292740	0.2932790	1.1009680
C	-1.5828050	5.5693400	1.5131590
C	-4.8658040	5.5250690	-0.3826170
C	-0.8573500	-5.5414680	-0.0074980
C	2.1770210	-3.8307150	0.8323820
H	-2.3332870	6.3141680	0.5377450
H	-0.6723580	5.7836070	2.1626800
H	-1.3499410	5.6986980	2.2815260
H	-4.1672000	5.8342520	1.4653100
H	-5.8121710	6.0503330	0.5035860
H	-1.4260250	-5.8375550	-0.4274640
C	0.0400730	-6.1576430	-1.2568970
H	-1.4740370	-5.7646930	-0.5828650
Mg	-1.2659480	0.1880890	-0.2137260
C	-6.9259120	-0.2137260	-0.1568350
H	-7.1277970	0.2336970	0.8206970
H	-7.1310100	0.5487480	-0.9130690
C	-7.6406850	-1.0256350	-0.3007320
H	-6.1311590	-3.8847220	0.8544130
H	-5.1813630	-4.1335620	1.3317520
H	-6.6619170	-3.1975070	1.5165750
O	-6.7214790	-4.8002400	0.7631660
H	2.7672420	-4.8859100	0.0683800
C	2.9655800	2.9078940	0.3192310
H	2.7641790	2.4483030	2.4077950
H	2.3071240	3.4022620	2.6763660
H	2.3251870	1.6760460	3.0441310
C	3.8339590	2.5049530	2.6264200
C	4.0776310	0.7905020	-0.6448090
H	5.4069570	1.4004630	-0.2295190
C	3.6294470	1.3566730	-1.4647060
H	4.2572180	-0.2154440	-1.0240590
C	6.3981790	1.5195360	-1.3550590
H	5.2760480	2.3977300	0.2012830
H	5.8692500	0.7896380	0.5519450
O	6.2323920	1.1699280	-2.4921580
O	7.5459200	2.0859650	-0.9278360
C	8.5644240	2.2301330	-1.9112720
H	8.2236850	2.8601350	-2.7341150
C	8.8561630	1.2585050	-2.3121580
C	-5.8933570	-3.2362670	-0.5126120
H	-6.8563610	-3.0113380	-0.9787960
H	-5.4005160	-3.9536280	-1.1741410
C	-4.5924270	4.5275060	0.6753350
H	-5.3514660	4.2374750	-0.0464500
C	2.9099480	-2.4324830	0.0502050
C	3.8213510	-2.3332930	1.2461980
O	5.0010010	-2.0863430	1.2067770
O	3.1559790	-2.5270730	2.3918860
C	3.9218690	-2.4225580	4.3982640
H	3.2270220	-2.6092510	3.5922710
H	4.7262770	-3.1591870	3.6776500
H	4.3554050	-1.4252070	-0.8315620
H	3.5509750	-2.3710760	-1.4018170
H	9.4047170	2.6958440	-3.3025590
C	-1.6982180	1.2518010	-4.3264060
H	-1.2674500	1.3424830	-2.5022820
O	-0.9644060	0.5852260	-3.0743530
O	-2.7798560	1.7797950	

Figure 8. **DFT optimized structure of Chl*a*-formate**

9

Chl*a*-formate ωB97XD/TZVP (ωB97XD optimized)

```
Excited State   1:      Triplet-?Sym    0.9778 eV 1267.98 nm  f=0.0000  <S**2>=2.000
     177 -> 179        -0.34358
     177 -> 180        -0.20181
     178 -> 179         0.61382
     178 -> 180        -0.15098
     177 <- 179        -0.14044
     177 <- 180        -0.12130
     178 <- 179         0.23231
This state for optimization and/or second-order correction.
Total Energy, E(TD-HF/TD-DFT) =  -2378.15541650
Copying the excited state density for this state as the 1-particle RhoCI density.

Excited state symmetry could not be determined.
Excited State   2:      Triplet-?Sym    1.5126 eV  819.69 nm  f=0.0000  <S**2>=2.000
     177 -> 179         0.60141
     178 -> 179         0.36003
     177 <- 179         0.13689

Excited state symmetry could not be determined.
Excited State   3:      Triplet-?Sym    2.1309 eV  581.83 nm  f=0.0000  <S**2>=2.000
     169 -> 179        -0.12362
     177 -> 180        -0.21222
     178 -> 180         0.62880

Excited state symmetry could not be determined.
Excited State   4:      Singlet-?Sym    2.1587 eV  574.33 nm  f=0.2049  <S**2>=0.000
     177 -> 179        -0.18273
     177 -> 180        -0.26541
     178 -> 179         0.61076

Excited state symmetry could not be determined.
Excited State   5:      Singlet-?Sym    2.4729 eV  501.37 nm  f=0.1064  <S**2>=0.000
     177 -> 179         0.59968
     178 -> 179         0.20354
     178 -> 180         0.27944
```

```
Excited State   6:   Triplet-?Sym    2.5028 eV  495.38 nm  f=0.0000  <S**2>=2.000
     167 -> 179         0.10066
     177 -> 179        -0.12063
     177 -> 180         0.57426
     177 -> 181         0.20623
     178 -> 179         0.13986
     178 -> 180         0.15515

Excited state symmetry could not be determined.
Excited State   7:   Triplet-?Sym    2.6805 eV  462.54 nm  f=0.0000  <S**2>=2.000
     171 -> 179        -0.13086
     173 -> 179         0.17072
     173 -> 180         0.10611
     174 -> 179         0.42900
     174 -> 180         0.27370
     174 -> 181        -0.17429
     174 -> 182        -0.10818
     175 -> 179        -0.17174
     176 -> 179         0.10527

Excited state symmetry could not be determined.
Excited State   8:   Singlet-?Sym    3.4059 eV  364.03 nm  f=0.6851  <S**2>=0.000
     174 -> 179         0.14789
     176 -> 179         0.11256
     177 -> 179        -0.25912
     177 -> 180        -0.10219
     178 -> 180         0.59771

Excited state symmetry could not be determined.
Excited State   9:   Singlet-?Sym    3.6027 eV  344.14 nm  f=0.7315  <S**2>=0.000
     175 -> 179         0.12555
     175 -> 180        -0.10620
     177 -> 180         0.58803
     178 -> 179         0.26695
     178 -> 180         0.10691

Excited state symmetry could not be determined.
Excited State  10:   Singlet-?Sym    3.6827 eV  336.67 nm  f=0.1748  <S**2>=0.000
     174 -> 179         0.26327
     176 -> 179         0.57142
     176 -> 180         0.10946
     178 -> 180        -0.13719
```

Figure 9. DFT energies of Chl*a*-formate

Table II. Transition energies and oscillator strength calculated for chl*a*-formate with Gaussian16 using TDDFT with the ωB97XD functional and TZVP basis. The structures are obtained at the same level of theory.
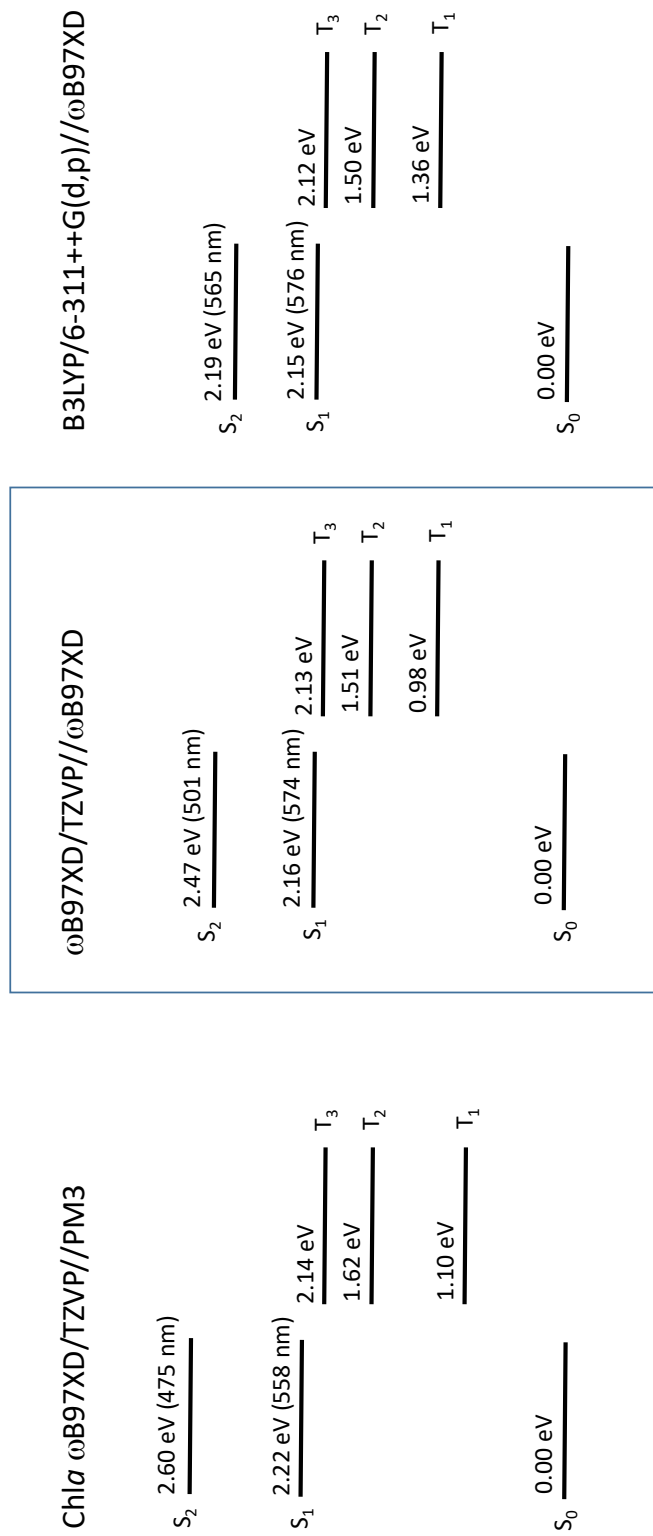
Excited State	Multiplicity	Transition Energy(eV)	Wavelength(nm)	Oscillator Strength
Excited State 4	Singlet	2.1587	574.33	0.2049
Excited State 5	Singlet	2.4729	501.37	0.1064
Excited State 8	Singlet	3.4059	364.03	0.6851
Excited State 9	Singlet	3.6027	344.14	0.7315
Excited State 10	Singlet	3.6827	336.67	0.1748
Excited State 1	Triplet	0.9778	1267.98	0.0000
Excited State 2	Triplet	1.5126	819.69	0.0000
Excited State 3	Triplet	2.1309	581.83	0.0000
Excited State 6	Triplet	2.5028	495.38	0.0000
Excited State 7	Triplet	2.6805	462.54	0.0000
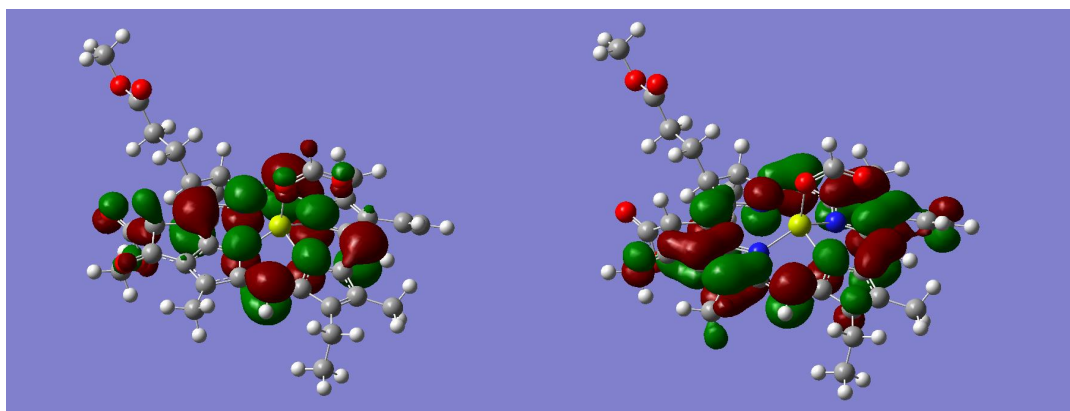
Homo orbital (178) of Chla-formate.   Lumo orbital (179) of Chla-formate.

Figure 10. **Molecular orbitals of Chl*a*-formate**

Chl*a* ωB97XD/TZVP//PM3

S$_2$ — 2.60 eV (475 nm)

S$_1$ — 2.22 eV (558 nm)

— 2.14 eV T$_3$
— 1.62 eV T$_2$

— 1.10 eV T$_1$

S$_0$ — 0.00 eV

ωB97XD/TZVP//ωB97XD

S$_2$ — 2.47 eV (501 nm)

S$_1$ — 2.16 eV (574 nm)

— 2.13 eV T$_3$
— 1.51 eV T$_2$

— 0.98 eV T$_1$

S$_0$ — 0.00 eV

B3LYP/6-311++G(d,p)//ωB97XD

S$_2$ — 2.19 eV (565 nm)

S$_1$ — 2.15 eV (576 nm)

— 2.12 eV T$_3$
— 1.50 eV T$_2$

— 1.36 eV T$_1$

S$_0$ — 0.00 eV

Results in the box are used for the SOC calculation

Figure 11. **Chl*a*-formate spectroscopy summary**

12

Spin-orbit coupling matrix elements

Output from the DFT calculations is used as input for a direct calculation of the spin-orbit coupling matrix elements using the PySOC code [5]. The needed files are obtained by adding required keywords to the Gaussian16 command line: TD(50-50,nstates=5) ωB97XD/TZVP 6D 10F nosymm GFInput.

Chl*a:* Spin-orbit matrix elements

sum_soc, <S0|Hso|T1,1,0,-1> (cm-1):	0.83854	0.20384	0.78743	0.20384
sum_soc, <S0|Hso|T2,1,0,-1> (cm-1):	0.24150	0.16776	0.04510	0.16776
sum_soc, <S0|Hso|T3,1,0,-1> (cm-1):	0.29307	0.16421	0.17878	0.16421
sum_soc, <S0|Hso|T4,1,0,-1> (cm-1):	0.16775	0.11013	0.06230	0.11013
sum_soc, <S1|Hso|T1,1,0,-1> (cm-1):	0.29407	0.03590	0.28965	0.03590
sum_soc, <S1|Hso|T2,1,0,-1> (cm-1):	1.28456	0.17647	1.26008	0.17647
sum_soc, <S1|Hso|T3,1,0,-1> (cm-1):	0.82038	0.13608	0.79749	0.13608
sum_soc, <S1|Hso|T4,1,0,-1> (cm-1):	0.20074	0.06257	0.18018	0.06257
sum_soc, <S2|Hso|T1,1,0,-1> (cm-1):	1.34659	0.19178	1.31899	0.19178
sum_soc, <S2|Hso|T2,1,0,-1> (cm-1):	0.12063	0.03691	0.10875	0.03691
sum_soc, <S2|Hso|T3,1,0,-1> (cm-1):	0.17280	0.00851	0.17238	0.00851
sum_soc, <S2|Hso|T4,1,0,-1> (cm-1):	0.76447	0.11951	0.74555	0.11951
sum_soc, <S3|Hso|T1,1,0,-1> (cm-1):	0.48741	0.06411	0.47890	0.06411
sum_soc, <S3|Hso|T2,1,0,-1> (cm-1):	0.10890	0.02564	0.10268	0.02564
sum_soc, <S3|Hso|T3,1,0,-1> (cm-1):	0.11532	0.01326	0.11379	0.01326
sum_soc, <S3|Hso|T4,1,0,-1> (cm-1):	0.15288	0.06664	0.12037	0.06664
sum_soc, <S4|Hso|T1,1,0,-1> (cm-1):	0.23425	0.15576	0.07972	0.15576
sum_soc, <S4|Hso|T2,1,0,-1> (cm-1):	0.30223	0.13594	0.23321	0.13594
sum_soc, <S4|Hso|T3,1,0,-1> (cm-1):	0.19544	0.08804	0.15065	0.08804
sum_soc, <S4|Hso|T4,1,0,-1> (cm-1):	0.02922	0.02066	0.00040	0.02066

Figure 12. **Spin-orbit matrix elements for Chl*a***

Chl*a*-formate*:* Spin-orbit matrix elements

```
sum_soc, <S0|Hso|T1,1,0,-1> (cm-1):    1.07855    0.26229    1.01276    0.26229
sum_soc, <S0|Hso|T2,1,0,-1> (cm-1):    0.41871    0.29583    0.01686    0.29583
sum_soc, <S0|Hso|T3,1,0,-1> (cm-1):    0.59081    0.41652    0.04563    0.41652
sum_soc, <S0|Hso|T4,1,0,-1> (cm-1):    0.10593    0.06569    0.05090    0.06569
sum_soc, <S1|Hso|T1,1,0,-1> (cm-1):    0.43386    0.05355    0.42720    0.05355
sum_soc, <S1|Hso|T2,1,0,-1> (cm-1):    1.33739    0.24912    1.29015    0.24912
sum_soc, <S1|Hso|T3,1,0,-1> (cm-1):    1.23704    0.25118    1.18494    0.25118
sum_soc, <S1|Hso|T4,1,0,-1> (cm-1):    0.20639    0.04781    0.19500    0.04781
sum_soc, <S2|Hso|T1,1,0,-1> (cm-1):    1.54275    0.28019    1.49099    0.28019
sum_soc, <S2|Hso|T2,1,0,-1> (cm-1):    0.20039    0.06825    0.17561    0.06825
sum_soc, <S2|Hso|T3,1,0,-1> (cm-1):    0.17840    0.09597    0.11579    0.09597
sum_soc, <S2|Hso|T4,1,0,-1> (cm-1):    0.92319    0.24115    0.85789    0.24115
sum_soc, <S3|Hso|T1,1,0,-1> (cm-1):    0.81866    0.16956    0.78276    0.16956
sum_soc, <S3|Hso|T2,1,0,-1> (cm-1):    0.28458    0.06107    0.27116    0.06107
sum_soc, <S3|Hso|T3,1,0,-1> (cm-1):    0.25315    0.03549    0.24813    0.03549
sum_soc, <S3|Hso|T4,1,0,-1> (cm-1):    0.23061    0.03030    0.22659    0.03030
sum_soc, <S4|Hso|T1,1,0,-1> (cm-1):    0.29243    0.07686    0.27148    0.07686
sum_soc, <S4|Hso|T2,1,0,-1> (cm-1):    0.71619    0.30286    0.57400    0.30286
sum_soc, <S4|Hso|T3,1,0,-1> (cm-1):    0.41746    0.05168    0.41101    0.05168
sum_soc, <S4|Hso|T4,1,0,-1> (cm-1):    0.12460    0.02907    0.11762    0.02907
```

Figure 13. **Spin-orbit matrix elements for Chl*a*-formate**

[1] S. P. Møller, Nucl. Instrum. Methods Phys. Res. Sec. A: Accelerators, Spectrometers, Detectors and Associated Equipment **394**, 281 (1997).

[2] L. H. Andersen, H. Bluhme, S. Boyé, T. J. Jørgensen, H. Krogh, I. Nielsen, S. Brøndsted Nielsen, and A. Svendsen, Phys. Chem. Chem. Phys. **6**, 2617 (2004).

[3] B. F. Milne, Y. Toker, A. Rubio, and S. Brøndsted Nielsen, Angew. Chem. Int. Ed. **54**, 2170 (2015).

[4] M. J. Frisch, G. W. Trucks, H. B. Schlegel, G. E. Scuseria, M. A. Robb, J. R. Cheeseman, G. Scalmani, V. Barone, G. A. Petersson, H. Nakatsuji, X. Li, M. Caricato, A. V. Marenich, J. Bloino, B. G. Janesko, R. Gomperts, B. Mennucci, H. P. Hratchian, J. V. Ortiz, A. F. Izmaylov, J. L. Sonnenberg, D. Williams-Young, F. Ding, F. Lipparini, F. Egidi, J. Goings, B. Peng, A. Petrone, T. Henderson, D. Ranasinghe, V. G. Zakrzewski, J. Gao, N. Rega, G. Zheng, W. Liang, M. Hada, M. Ehara, K. Toyota, R. Fukuda, J. Hasegawa, M. Ishida, T. Nakajima, Y. Honda, O. Kitao, H. Nakai, T. Vreven, K. Throssell, J. A. Montgomery, Jr., J. E. Peralta, F. Ogliaro, M. J. Bearpark, J. J. Heyd, E. N. Brothers, K. N. Kudin, V. N. Staroverov, T. A. Keith, R. Kobayashi, J. Normand, K. Raghavachari, A. P. Rendell, J. C. Burant, S. S. Iyengar, J. Tomasi, M. Cossi, J. M. Millam, M. Klene, C. Adamo, R. Cammi, J. W. Ochterski, R. L. Martin, K. Morokuma, O. Farkas, J. B. Foresman, and D. J. Fox, "Gaussian16 Revision C.01," (2016), gaussian Inc. Wallingford CT.

[5] X. Gao, S. Bai, D. Fazzi, T. Niehaus, M. Barbatti, and W. Thiel, J. Chem. Theory Comput. **13**, 515 (2017), https://doi.org/10.1021/acs.jctc.6b00915.